Combustion and Flame 196 (2018) 45–53

Contents lists available at ScienceDirect

Combustion and Flame

journal homepage: www.elsevier.com/locate/combustflame

# A theoretical kinetics study on low-temperature reactions of methyl acetate radicals with molecular oxygen

Qinghui Meng[a,b], Xudong Zhao[a], Lidong Zhang[a,*], Peng Zhang[b,*], Liusi Sheng[a]

[a] National Synchrotron Radiation Laboratory, University of Science and Technology of China, Hefei, Anhui 230029, PR China
[b] Department of Mechanical Engineering, the Hong Kong Polytechnic University, Hong Kong, Hong Kong

ARTICLE INFO

*Article history:*
Received 8 January 2018
Revised 5 February 2018
Accepted 22 May 2018
Available online 23 June 2018

*Keywords:*
Methyl acetate
RRKM
Master equation
Low-temperature oxidation
Biodiesel

ABSTRACT

Theoratical studies on the chemistry of methyl acetate radicals with molecular oxygen was conducted to get further understanding of biodiesel combustion. Reactions of the first oxygen addition to methyl acetate radicals has been investigated by high level quantum chemical methods, and rate constants were computed by using microcanonical variational transition state theory coupled with Rice–Ramsberger–Kassel–Marcus/Master-Equation theory. The calculated rate constants agree reasonably well with both theoretical and experimental results of chain-like alkoxy radicals. We considered each step in the oxidation process as a class of reaction, including all the possible reactions taking place, only the formation and re-dissociation of initial adducts are critical for the low temperature combustion of methyl acetate. The current study is an extension of kinetic data for such chain propagation reactions for methyl acetate oxidation in a wider pressure and temperature range, which can be used for the modeling study of low temperature oxidation of methyl esters.



## 1. Introduction

Biodiesel, as an environment friendly source of renewable energy, has been regarded as one of the most promising alternative fuels [1–3]. The main component of biodiesel is esters, which contain oxygen in their molecular structure and can be obtained from several types of oil, including soybean oil in the United States and rapeseed in Europe [4]. Esters are typically made of long (16–18) carbon atom chains and usually require very large detailed chemical kinetic models to precisely describe their oxidation. Compared with the combustion of fossil fuels, combustion of biodiesels could effectively reduce soot formation by suppressing its precursors in combustion processes [5], mitigating the climatic impact of fuel combustion. The detailed kinetic study of biodiesel is challenging both experimentally and theoretically because of the complexity and the size of the biodiesel components. As a result, surrogate molecules are widely used in kinetic studies to imitate the property of real biodiesel [6]. Some small molecules, such as methyl formate, methyl acetate (MA), methyl crotanoate, and methyl butanoate (MB), which are usually chosen to investigate the chemical kinetics of the characteristic ester moiety, have instead served as surrogates of biodiesels in combustion research [5,7–10].

MA is the simplest methyl ester with a chain only one carbon atom connected to the methyl ester group. And it is also an important reaction intermediate during the pyrolysis of biodiesel and a potential pollutant of the atmospheric degradation. Furthermore, association reactions of MA radicals and $O_2$ reaction represent an important model system to explore the kinetic consequences of the methyl ester radical oxidation; it contains many of the complexities of larger systems, yet is more feasible to detailed electronic structure calculations.

Regardless of the extensive research on developing elementary reactions for the high temperature oxidation and pyrolysis [11–13], only a few studies have been performed to promote the development of low-temperature combustion sub-mechanisms for methyl esters. It remains experimentally challenging to obtain reliable rate constants regarding biodiesel autoignition at low temperature due to the inherent complexity of chain reactions of ROO radicals formed by reactions between R with $O_2$. Low-temperature kinetics plays important role in the combustion of biofuel homogeneous charge compression ignition (HCCI) engines employing biofuels. Under normal HCCI conditions, the formation of combustion pollutants occur in a relatively low-temperature the formation of pollutants is believed to occur in the relatively low temperature regions of the combustion chamber. Thus, the low-temperature

* Corresponding authors.
*E-mail addresses:* zld@ustc.edu.cn (L. Zhang), pengzhang.zhang@polyu.edu.hk (P. Zhang).

https://doi.org/10.1016/j.combustflame.2018.05.023
0010-2180/

oxidation processes is crucial in reducing $NO_x$ and soot emissions and increasing combustion efficiency.

In the development of biodiesel reaction mechanisms, Dooley et al. [14] neglected the low-temperature oxidation of methyl ester peroxy radicals since its reactivity was assumed to be less relevant to a shock tube and rapid compression machine auto-ignition measurements. However, the rapid compression machine results suggested that reactions of $O_2$ addition to biodiesels have great influence on the combustion behavior at the low-to-intermediate temperature range (770–950 K). Recently, Zádor et al. [15] reviewed the low-temperature chemistry in an article and concluded that development of biofuel combustion modeling, given its potential significance, has been limited to the availability of detailed knowledge of dissociation and isomerization processes relevant to auto-ignition in oxygenated alkyl peroxy radicals.

Until recent years, researchers started to pay more attentions to the combustion mechanisms of the low-temperature oxidation of biodiesels. The first study of the low temperature oxidation of MA was performed by Dagaut et al. [16] in a jet-stirred reactor (JSR) at the temperature ranging from 800 to 1230 K and at the pressure of 10 atm. A comprehensive kinetic mechanism, largely based on the structure-reactivity of methyl acetate and related species including ethane, methanol, and dimethyl ether, was developed to interpret their experiments. The JSR results indicate that of the early reaction and the increase of CO formation are sensitive to the branching propagation reactions in low temperature oxidation of MA. A theoretical study of low-temperature oxidation of MB was conducted by Tao and Lin [17], in which reaction channels and thermochemistry of methyl ester peroxy radical decomposition has been analysed by the DFT method. Rate constants in the kinetic sub-mechanism were calculated by using the canonical transition state theory. However, the kinetic parameters for barrierless reactions of the $O_2$ addition to MB radicals, which are the entrance channels on the corresponding potential energy surface, were not considered. Jiao et al. [18] also investigated the auto-ignition of MB theoretically by employing the composite CBS-QB3 method, and their study focused on the quantum chemistry and kinetics of isomerization and decomposition reactions initiated by hydroperoxy methyl ester radicals formed in second $O_2$ addition reactions to MB peroxy radicals. The kinetic study of methyl acetate pyrolysis and oxidation was conducted experimentally and theoretically by Yang et al. [19]. Rate constants of the hydrogen abstraction and subsequent radical decomposition reactions for MA were calculated by high-level ab initio and RRKM master equation methods. The developed model by Yang et al. [19] was validated against experimental results from an atmospheric flow reactor and a low-pressure flat flame using molecular beam mass spectrometry. Deka and Mishra [20] developed a kinetic mechanism where the rate coefficient of the H-atom abstraction of MA by chlorine atoms was computed by using G2(MP2)//MPWB1K/6-31 + G(d,p) method and RRKM master equation analysis at 298 K. Tan et al. [21] also, respectively, conducted theoretical studies on the H-atom abstraction of MA initiated by free radicals (H, OH, $HO_2$, $CH_3$ and O), whose predications were validated against available theoretical results reported previously [11,22].

Although the elementary reactions of the $O_2$ addition to MA radicals and the following isomerization and decomposition reactions of MA peroxy radicals are critical to determine the low-temperature auto-ignition, few studies has been done to focus on the sub-mechanism of low-temperature oxidation for MA. The ignition of MA is mainly initiated by hydrogen abstraction with free radicals to form one of two carbon centerd radicals: $\cdot CH_2COOCH_3$ (denoted by MA2J) and $CH_3COOCH_2\cdot$ (denoted by MAMJ). The MA radicals can isomerize to each other via 1, 4-H shift. Under low temperature range, MA radicals can directly react with $O_2$ and then form peroxy radicals. These peroxy radicals can isomerize to hydroperoxy alkyl radicals (·QOOH), which in turn can decompose through concerted OH-loss or $\beta$-scission and can reverse to the peroxy radicals. The OH-loss and $\beta$-scission reactions involving ·QOOH either propagate the radical chain reaction or lead to radical chain branching. These reactions have a great influence on the low-temperature combustion chemistry of MA. Compared with the analogous alkyl reaction systems, the present system is more complicated because of the presence of the oxygenated ester group.

In the manuscript, MA is recognized as a candidate methyl ester for surrogate formulation and is also considered as the starting point for the development of reaction rate rules and kinetic mechanism of other methyl esters. For the present work, we identified detailed reaction pathways for each radical and determined the potential energy surfaces (PES) by using highly accurate theoretical methods. Rate constants were subsequently calculated for dominant channels. Master equation analysis of the kinetics for barrierless reactions was performed to obtain accurate temperature- and pressure-dependent rate constants. Moreover, phenomenological rate coefficients and competing relationship among reaction pathways were provided for this system to develop the chemical kinetic modeling of low temperature oxidation of methyl esters. A detailed kinetic model of reactions of MA peroxy radicals and QOOH has been described in the present study which is also compared with MB peroxy radicals reported in early studies [17].

## 2. Theoretical methodology

### 2.1. Electronic structure calculations

The method of M06-2X/cc-pVTZ was employed in the geometry optimization and frequency analysis of stationary points on the MAOO potential energy surfaces [23]. Transition states possessing one and only one imaginary frequency were verified to correspond to desired reaction coordinates via visual inspections. For ambiguous cases, the intrinsic reaction path analysis was utilized to examine the connections of each saddle point to its local minima. Vibrational frequencies were scaled by a factor of 0.985 [24], and the zero-point energies (ZPE) were obtained at M06-2X/cc-pVTZ level. High level single-point energies of these species were corrected by using two high-level theories. The first one is the coupled-cluster singles and doubles with perturbative triples correction (CCSD(T)) theory implemented in Molpro package [25]. The single-point energies were obtained by restricted CCSD (T) with cc-pVXZ (X = D, T) basis sets [26]. The second is the explicitly-corrected CCSD(T)-F12 method [27] implementation in the same package [25]. The extrapolation of F12 correlation energies can be highly accurate even with just a DZ/TZ pair of basis sets [27]. Energy extrapolation to the complete basis set (CBS) limit was conducted with two-point extrapolation scheme [26,27]:

$$\begin{aligned}&E[CCSD(T)/CBS]_{DZ\rightarrow TZ}\\&= E[CCSD(T)/cc-pVTZ] + \{E[CCSD(T)/cc-pVTZ]\\&\quad - E[CCSD(T)/cc-pVDZ]\} \times 0.4629\end{aligned} \tag{E1}$$

$$\begin{aligned}&E[CCSD(T)-F12/CBS]_{DZ\rightarrow TZ}\\&= E[CCSD(T)-F12/cc-pVTZ] + \{E[CCSD(T)-F12/cc{-}pVTZ]\\&\quad -E[CCSD(T)-F12/cc-pVDZ]\} \times 0.4210\end{aligned} \tag{E2}$$

The molecular oxygen with triple ground state reacts like radicals in the entrance channel of $O_2$ addition reactions that are typically barrierless. Single reference methods failed to deal with this process. The multi-reference method CASSCF(7e,5o)/cc-pVDZ-F12 was employed for frequency calculations and the relaxed scan along the reaction coordinate. The frequencies of the initial formed

adduct obtained by the M06-2X/cc-pVTZ method were chosen as reference to calculate the scaled factor of CASSCF(7e,5o)/cc-pVDZ-F12 method. Thus, all the frequencies along the MEP for $O_2$ addition to the radical needed for VTST calculations were obtained by the multi-reference method with a specific scaled factor 0.984. The active space was chosen as (7e, 5o) including six electrons in two pairs of O–O $\pi$ and $\pi^*$ orbitals and one electron in a radical orbital. After that, the explicitly correlated multi-reference configuration interaction (MRCI-F12) method combined with the cc-pVDZ-F12 basis set was used to map out the minimum energy pathway (MEP) [28]. When combined with cc-pVDZ-F12 orbital auxiliary basis sets, recently developed F12 methods utilize an exponential correlation factor, which can achieve results near aug-cc-pVQZ quality with a negligible increase in computation load [29,30]. The energy obtained above were scaled asymptotically by referring to corresponding energies of the $O_2$ addition reactions achieved at CCSD(T)/CBS//M06-2X/cc-pVTZ level.

For the barrierless channels in this case, the CASPT2 method is unable to predict smooth energy potentials due to the existence of strong interactions between O and H atoms. An H atom could even be abstracted by $O_2$ with these two atoms getting close to each other, which is also found in previous studies [31]. Thereby, the potential calculations by using the MRCI-F12(7e,5o)/cc-pVDZ-F12 //CASSCF(7e,5o)/cc-pVDZ-F12 were chosen for the $O_2$ addition channels. In addition, the geometries, energies and frequencies of the variational transition states in barrierless reactions of MAMJ + $O_2$ were also calculated by using the CASPT2(7e,5o)/ cc-pVDZ-F12 method for comparison.

All the present DFT calculations were performed by using the Gaussian 09 program suite [32]; multi-reference calculations were performed by using the Molpro 2010 program package [25].

### 2.2. Rate constant calculations

The pressure-dependent rate coefficients were computed by solving the time-dependent master equations based on RRKM theory [33] through employing the MESS code [34]. The collisional energy transfer was approximated by a single-exponential-down model, $(\Delta E)_{down} = 250(T/300\,K)^{0.85}$, which has been validated in relevant studies of MB [35] and n–butyl radicals [36]. Rate constant calculations were performed for wide ranges of temperatures from 300 to 1500 K and pressures from 0.01 atm to 10 atm. The interaction between reactant and bath gas Argon was estimated by using the Lennard–Jones (L–J) model. The L–J parameters of Ar, $\sigma = 3.47$ Å and $\varepsilon = 79.2$ cm$^{-1}$, were adopted from the early literature [37]. For methyl acetate radicals, the L–J parameters, $\sigma = 5.94$ Å and $\varepsilon = 669.8$ cm$^{-1}$, were calculated by using the empirical method of Chung et al. [38,39].

For the channels with pronounced transition states, the high-pressure rate constants were computed by using the conventional transition state theory (CTST) applying the rigid-rotor harmonic-oscillator (RRHO) assumption for all degrees of freedom except for the torsional modes. The low-frequency torsional modes corresponding to internal rotations were simulated as one-dimensional (1-D) hindered rotors with hindrance potentials, which were obtained by a relaxed scan with the increment of 10 degrees at the M06-2X/cc-pVTZ level. As reactions considered in the consumption of MD radicals involving the transfer of hydrogen atoms, the tunneling effect on the rate constants was calculated on base of asymmetric Eckart model [40].

On MAOO surfaces, the $O_2$ addition reaction to MA radicals has a loose transition state along the reaction coordinate and the microcanonical variational transition state theory (μVTST) was implemented to evaluate the minimum number of states at each specific energy for the transition states [41,42]. The most distinctive feature of μVTST approach lies in that the optimal dividing surface, which is devised to minimize the rate flux from reactants to products, is a function of energy [43,44]. This procedure for computing variational TST rate constants was proposed by da Silva and Bozzelli [45]. As described above, the interaction potentials predicted by MRCI-F12(7e,5o)/cc-pVDZ-F12//CASSCF(7e,5o)/cc-pVDZ-F12 were used in the variation treatment of transition state theory.

**Table 1**
Comparison of the relative energies of various reaction channels calculated at 0 K by CCSD(T) and CCSD(T)-F12 methods.

| | $E_{CCSD(T)/CBS}$ (kcal/mol) | $E_{CCSD(T)-F12/CBS}$ (kcal/mol) |
|---|---|---|
| $\cdot CH_2COOCH_3 + O_2 \rightarrow \cdot OOCH_2COOCH_3$ | 24.33 | 24.46 |
| $CH_3COOCH_2\cdot + O_2 \rightarrow CH_3COOCH_2OO\cdot$ | 32.94 | 33.13 |
| $\cdot OOCH_2COOCH_3 \rightarrow HOOCH_2COOCH_2\cdot$ | 31.23 | 31.15 |
| $CH_3COOCH_2OO\cdot \rightarrow \cdot H_2CCOOCH_2OOH$ | 33.57 | 33.85 |

## 3. Results and discussion

### 3.1. Electronic structure calculations

The MAOO radicals were generated from MA radicals with molecular oxygen via barrierless reaction channels. Optimized geometries, rotational constants and vibrational frequencies of all the species are given in the Supplementary material. Table 1 display the well depth of the formation for MAOO adducts and their energy barriers of isomerization at 0 K for the different $O_2$ addition reactions. Two independent theories of CCSD(T) and CCSD(T)-F12 were utilized to calculate the single-point energies of all the species, and the results are almost the same between the two theories. Considering the calculation accuracy and computation cost, the PESs were constructed by using CCSD(T) theory. The M06-2X/cc-pVTZ optimized structures for the MAOO complexes produced by the addition of $O_2$ to MA radicals are illustrated in Fig. S1. The lowest energy conformer of each MAOO radicals was identified as the local minimum though relaxed potential scans. These conformations were used as starting points when interaction potentials of barrierless reactions were explored by using MRCI-F12 methods implemented in Molpro [25].

The PES for the major reaction channels at the CCSD(T)/CBS//M06-2X/cc-pVTZ level is shown in Fig. 1. The well depths of the initially-formed adducts, such as MA2JOO and MAMJOO are 24.33 and 32.94 kcal/mol, respectively. The energy barrier of MA2J is significantly lower than that of MAMJ owing to the presence of –C(·)–C=O conjugated system in the MA2J radical, which reduces the energy of MA2J + $O_2$ and therefore has different reaction behaviors. The well depth of MAOO· adduct determines how the re-dissociation channel competes with other decomposition reaction channels of MAOO. The initial adduct MA2JOO isomerizes to form $CH_2(OOH)C(=O)CH_2\cdot$ (i.e. W2 in Fig. 1) through a 7-membered-ring transition states with a barrier energy of 31.23 kcal/mol, which is higher than that of the re-dissociation of MA2JOO radicals (i.e. W1 in Fig. 1). Thus the re-dissociation of MA2JOO is more competitive that the isomerization. The MA2JOO adduct also can isomerizes to form $CH\cdot(OOH)C(=O)OCH_3$ via 1,3-H shift with a barrier of 40.38 kcal/mol (a relatively high energy), so its contribution to products is negligible. The intermediate W2, having the relative energy of −15.13 kcal/mol, can undergo $\beta$-scission to form $HOOCH_2C\cdot(=O)$ (i.e. P3 in Fig. 1) simultaneously releasing a formaldehyde with a relative high barrier of 36.39 kcal/mol, this dissociation channel plays a less important role in the low-temperature oxidation of MA. The formation of $OCH_2C(=O)OCH_2OH$ (i.e. P4 in Fig. 1) goes through the OH-migration from MA2JOO with the high barrier of 40.38 kcal/mol.

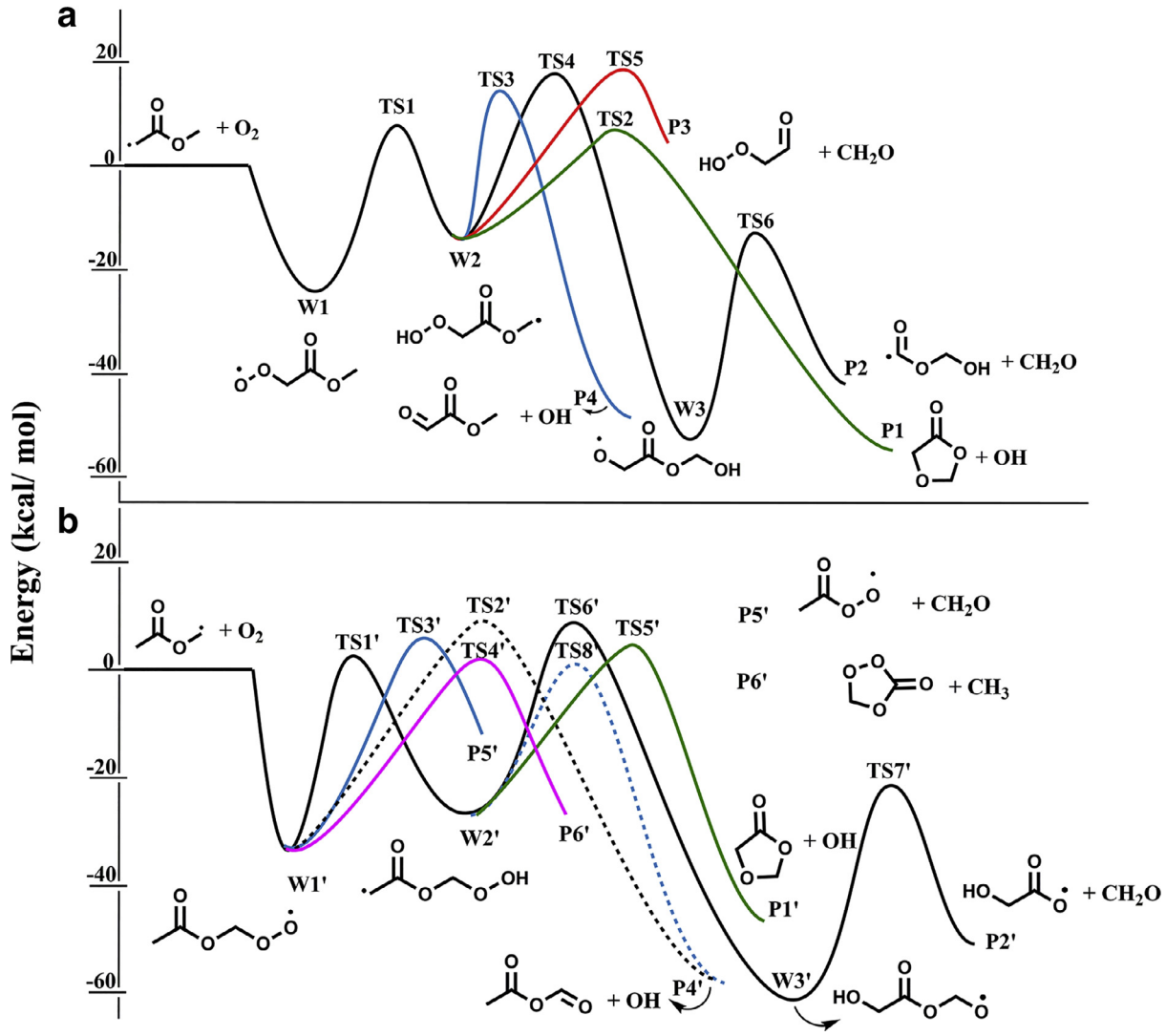


**Fig. 1.** Potentials energy surfaces for the methyl acetate radicals with $O_2$ at the CCSD(T)/CBS//M06-2X/cc-pVTZ level (a) MA2J + $O_2$ and (b) MAMJ + $O_2$.

Even the product of OH-migration channel has a low relative energy, this channel is less important. Alternatively, the intermediate W2 can dissociate to form $CH(=O)C(=O)OCH_3 + OH$. The lowest energy reaction channel of this system is the formation of cy[$OCH_2C(=O)OCH_2$] via a 5-membered-ring transition state involving O–O bond breaking and C–O bond forming, with a barrier height of 21.18 kcal/mol.

For MAMJ + $O_2$ reaction system, the well depth of MAMJOO adduct formation is 32.94 kcal/mol lower than the reactants which are closer to those of MB system [17]. Two different products: cy[$C(=)OCH_2OO$](P6′) + $CH_3$·, $CH_2C(=O)OO$· (P5′) + $CH_2O$ can be directly formed from the initial adduct through ring TS, with barrier of 33.44 and 35.90 kcal/mol, respectively. The MAMJOO(W1′) can isomerize to form $CH_2C(=O)CH_2OOH$(W2′) via 1,6-H shift and $CH_3C(=O)OCHOOH$ via 1,3-H shift with the barrier of 33.86 and 42.29 kcal/mol, respectively. The product of this 1, 3-H shift isomerization is unstable and easily dissociate to form $CH_3C(=O)OCHO$(P4′) + OH. The $CH_2C(=O)CH_2OOH$(W2′) can dissociate to form cy[$OCH_2C(=O)OCH_2$](P1′) + OH and P4′+OH, with barrier of 27.74 and 30.57 kcal/mol, respectively. These four reaction channels are more favored due to the lower barrier. A more detailed discussion can be found in rate constant analysis. These molecular properties of methyl acetate radical system can be applied to similar methyl ester oxidation systems in the later related studies.

Although previous studies have indicated that methyl ester with aliphatic chain less than five C atoms is not ideal surrogate to simulate biodiesel combustion, this theoretical study on the MA is helpful to understand the chemical kinetic of the ester moiety, a characteristic functional group of biodiesel components. In addition, the structure reactivity relationships of the low temperature oxidation of biodiesels can also be abstracted from a series studies. Actually, isomerization reaction in methyl acetate peroxy radicals cannot transferable to larger methyl esters due to the strong conjugation effect.

### 3.2. High-pressure limit rate constants

Because of the paucity of kinetics data of methyl acetate, only comparisons with previous high-pressure rate constants of chain-like radicals were made for the present system. Only the kinetically preferred reaction pathways discussed above were taken into consideration for rate constant calculations.

Figure 2 represents the present prediction of high pressure limit rate constants for the $O_2$ addition to methyl acetate radicals by using the variational transition state theory. From the plots, addition reactions of $O_2$ to methyl acetate radicals show positive temperature dependence, which is also reported in the reaction of ethyl and $O_2$ by Miller et al. [41]. The recombination rate constant of MAMJ + $O_2$ is higher than that of MA2J + $O_2$ since the well depth of

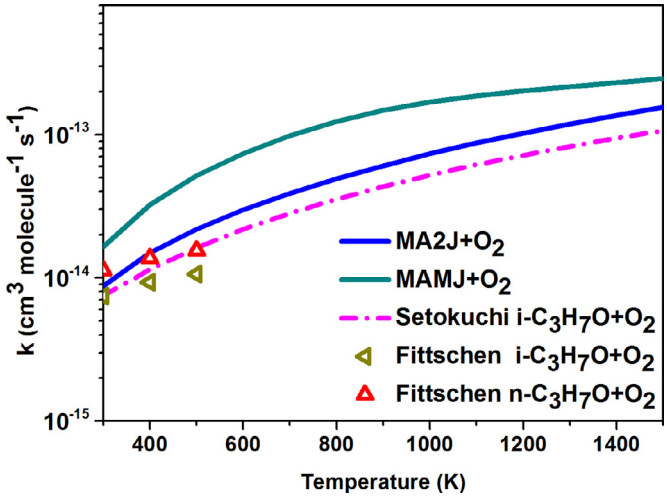


**Fig. 2.** Rate constants for MA· + $O_2$→MAOO at high pressure limit (HPL). The HPL rate constants of the association reaction for chain-like alkoxy radicals are form previous study [46,47].

MAMJ (32.94 kcal/mol) is larger than that of MA2J (24.33 kcal/mol). The recombination rate constant of the MAMJ + $O_2$ show slightly positive temperature dependence. At low temperatures, the variational transition state locates at longer C–O distance, where the MEP has a smaller slope and the enthalpy change dominates the temperature dependence. As temperature increases, the transition state lies at shorter C–O separation where the MEP has a larger slope and the decreasing entropy dominates the temperature dependence. For $O_2$ addition to the MAMJ, the rate constants are larger than those of MA2J in the important range of low temperature (500–800 K), which displays weaker temperature dependence. Due to the uniqueness of methyl acetate and scarcely available data, rate constants of low oxidation reactions for ether [46] and ethyl [41] were illustrated for comparison. The low-temperature oxidation kinetic data of n- and i-propoxy radicals and $O_2$ have been measured by Fittschen et al. [47] though experimental detection, which are in generally good agreement with our results at temperature between 300 and 500 K. In addition, association rate constants of i-propoxy radicals and $O_2$ explored by Setokuchi and Sato [46] on base of the high-level ab initio theory and the variational transition state theory, agree well with the present calculations at temperature ranging from 300 to 1500 K.

It is noted that the association rate constants of ethyl and $O_2$ show the similar temperature-dependence trend with that of methyl acetate radicals and $O_2$, while the difference is as high as three orders of magnitude [41]. The rate constants of the entrance channel association are seemed too low and a detailed analysis is required to understand the deviation. Thus, the shape of the entrance channel minimal energy potential (MEP) and analysis of the energies, geometries and frequencies of the variational transition states are discussed as follows.

For the barrierless reactions of MA2J + $O_2$, the pi bond in the carbonyl group overlaps with adjacent p orbitals of MA2J radicals, whose electron of interaction associated with conjugation effect is comparable with allyl radicals. Thus, the high-pressure limit rate constant of MA2J + $O_2$, i-$C_4H_5$($CH_2$=C=$CHCH_2$) + $O_2$ [49] and allylic isobutenyl radical ($CH_2$=C(CH)$CH_3$) + $O_2$ [50] are shown in Fig. 3(a) to depict the conjugation effect on the rate constants. The comparison shows that the rate constants exhibit good agreement with each other and the maximum deviations are within a factor of 3 at high temperatures. Compared with alkane radicals, the smaller rate constants of barrierless reactions for the methyl acetate and the

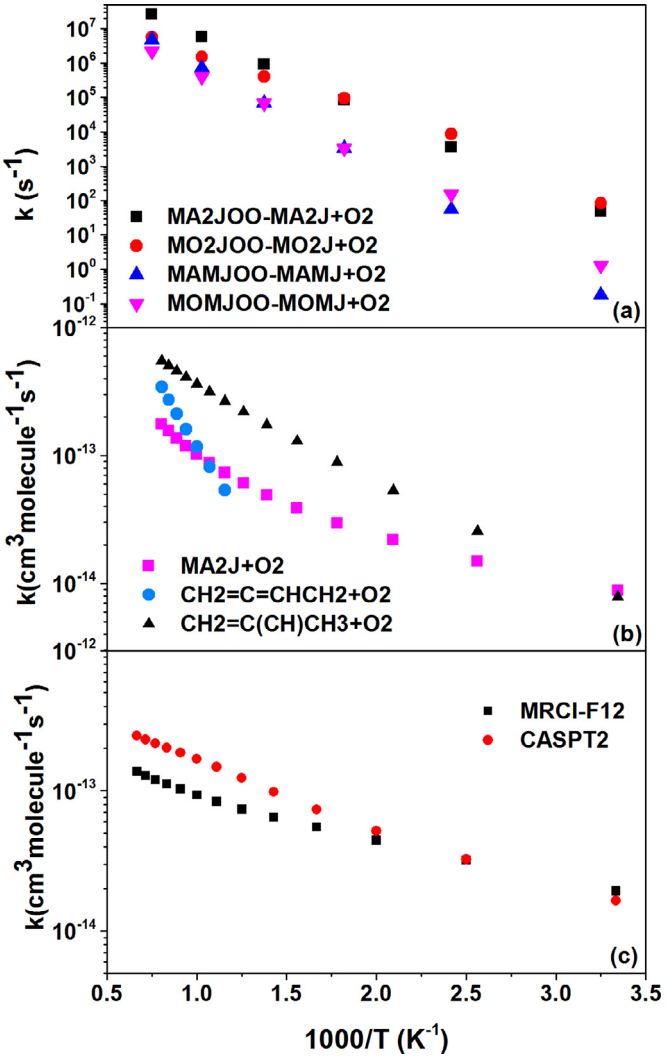


**Fig. 3.** The high-pressure limit rate constants of (a) the barrierless reactions of MA2J + $O_2$, i-$C_4H_5$($CH_2$ = C = $CHCH_2$) + $O_2$ [49] and allylic isobutenyl radical ($CH_2$ = C(CH)$CH_3$) + $O_2$ [50], (b) the barrierless reactions of MAMJ + $O_2$ by using the MRCI-F12 and CASPT2 methods and (c) the unimolecular reactions of methyl acetate and methyl octanoate peroxy radcials [51].

allyl radicals are attributed to their smaller entropies as a result of the strong conjugation effect.

Another suspicion is that the low rate constant could be an artifact of the use of CASSCF frequencies, which are generally unreliable. Since the system has only 9 atoms, CASPT2 frequency calculations should provide more reliable results than CASSCF. For the barrierless reactions of MAMJ + $O_2$ radicals, the MRCI-F12(7e,5o)/cc-pVDZ-F12//CASSCF(7e,5o)/cc-pVDZ-F12 and CASPT2/cc-pVDZ-F12 methods were employed to calculate the energies, geometries and frequencies of the variational transition states. In addition, the Davidson corrections for quadruple excitations were included in the MRCI-F12 calculations. The high-pressure limit rate constants of the barrierless reaction of MAMJ + $O_2$ by the MRCI-F12 and CASPT2 methods were displayed in Fig. 3(b). The calculated rate constants by these methods are in excellent agreement. The geometries with low entropies of the variational transition state are the main reason for the low rate constant of the barrierless reactions. As the methyl acetate radicals with carbonyl group, the conjugation and steric effects make the O atom in triplet oxygen tend to bond with the C atom in the carbonyl group. A tight complex associated with low entropy

is produced when the O atom in oxygen attacks the $CH_2$ group. The electron interaction between O atom and C atom in the carbonyl group was also identified by the relaxed scan along the fixed C–O bond. The longer distance between O atom in oxygen and C atom in the $CH_2$ group, the more significant is the tendency. As well as the association reaction of MAMJ and $O_2$ with resonance interaction has swallower well depth than that of ethyl systems by 1.1 kcal/mol [41], the smaller entropic change in MA peroxy radicals are largely responsible for the significant difference of the $O_2$ addition reaction between acethane and MA systems.

As described in the introduction, theoretical studies on the first $O_2$ addition to methyl ester radicals have been extensively conducted in recent years. However, the rate constants of the $O_2$ addition (barrierless) reactions were either determined by analogy to alkanes or simply neglected. To our best knowledge, the only rate constants of unimolecular reactions of methyl octanoate peroxy radicals were presented very recently [51]. Figure 3(c) compares the high-pressure limit rate constants of the unimolecular reactions of methyl acetate and the methyl octanoate peroxy radicals. It is seen that the decomposition rate coefficients of methyl acetate peroxy radicals are in fair agreement with their counterparts of methyl octanote peroxy radicals.

Eventually, the low rate constants of the entrance channel of the $O_2$ addition to methyl acetate radicals were identified to be reliable and physically correct by analysing the energies, geometries and frequencies of the variational transition states and being compared with available data. The minimum energy pathways along the C–O bond of the barrierless reactions for methyl acetate radicals obtained by using the MRCI-F12(7e,5o)/cc-pVDZ-F12 method were demonstrated in Fig. S2 of the Supplementary material.

### 3.3. Pressure-dependent rate constants

It is recognized that reaction mechanisms of ROO radicals have significant effect on the autoignition behavior of biodiesels [15]. In the present problem, the temperature and pressure-dependent rate constants are sensitive to the well depth of the MAOO formation. Figure 4 plots recombination rate constant of MAOO + $O_2$ at different pressures. Below 600 K, the calculated rate constants show weak pressure dependence, while significant pressure dependence was observed with temperature increase. For example, rate constants show a factor of 2 orders of magnitude deviation at 0.01 atm and 1000 K, comparing with that of high pressure limit. At 0.01 atm, absence of rate constants at temperature above about 1000 K is explained by the fact that the MA2JOO equilibrates with W1 more rapidly than its collisional energy transfer. There is a fall-off at finite pressures as the stabilization reaction equilibrates, and the onset temperature increases with the pressures. The complex behavior is attributable to the dissociation mechanism of MAOO to MA + $O_2$.

Intramolecular hydrogen transfer is a key step for low-temperature oxidation reactivity of fuels. Figure 5 demonstrates rate constants and of isomerization reactions for MA radicals, with relevant data of MB and dimethyl ether for comparison. In the present system, the products of 1, 3-H shift with relatively high barrier height is hard to proceed, and therefore only the kinetic parameters of 1, 6-H shift for MAOO radicals were considered in this manuscript. The rate constant of 1, 6-H shift for MA2JOO is higher than that of MAMJOO by a rough factor of 10 due to the lower energy barrier. As shown in Fig. 5, the calculated rate constants of isomerization reactions for MBOO are in excellent agreement with the theoretical data predicted by using G3MP2B3//B3LYP/6-31G(d)method [17], while the significant discrepancy of isomerization reactions from methyl ester peroxy radicals in MB and MA was observed at low temperature. At temperature below 800 K, kinetic difference between 1, 6-H migration reactions of MBMJOO

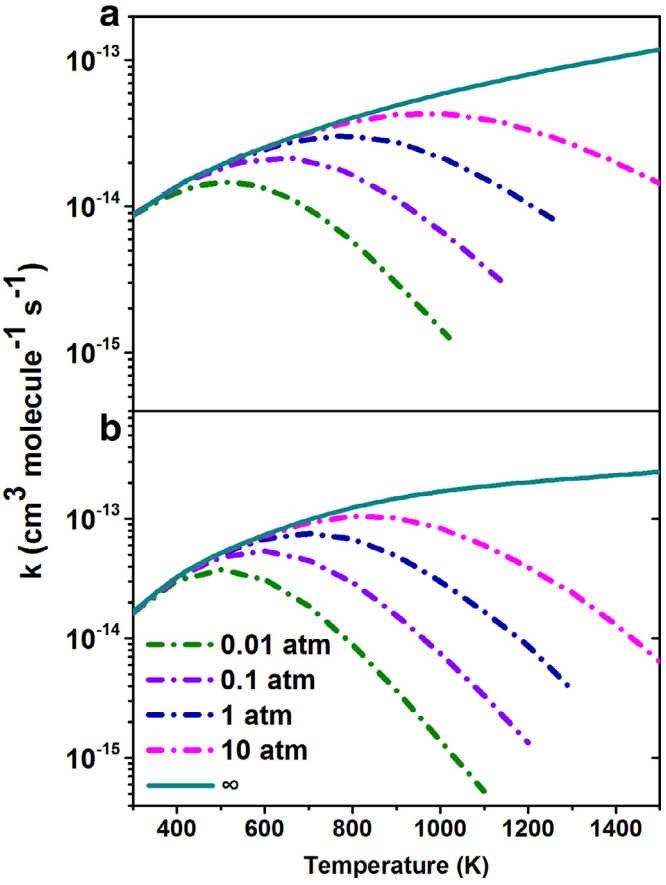


**Fig. 4.** Rate constants for MA· + $O_2$→MAOO at various T/P regimes. (a) $CH_2C(=O)OCH_3 + O_2$ and (b) $CH_3C(=O)OCH_2· + O_2$.

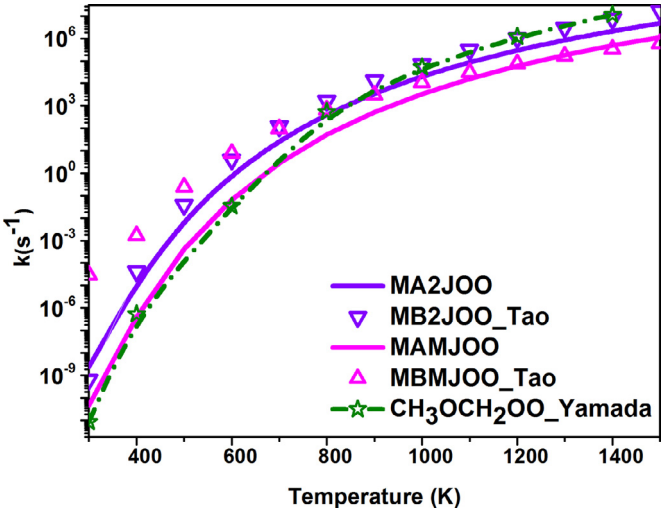


**Fig. 5.** Rate constants of H-migration reactions for MAOO radicals at high pressure limit. The rate constants of isomerization for chain-like peroxyl radicals are represented by different symbols.

and that of MAMJOO is as high as 5 orders of magnitude, which is caused by the fact that MBMJOO isomerization reaction with barrier height of 29 kcal/mol is roughly lower than that of MAMJOO by 4 kcal/mol. In addition, the rate constant of MAMJOO isomerization reaction has a good agreement with that of dimethyl ether peroxy adduct, which has an O atom in the ring-structure transition state [48].

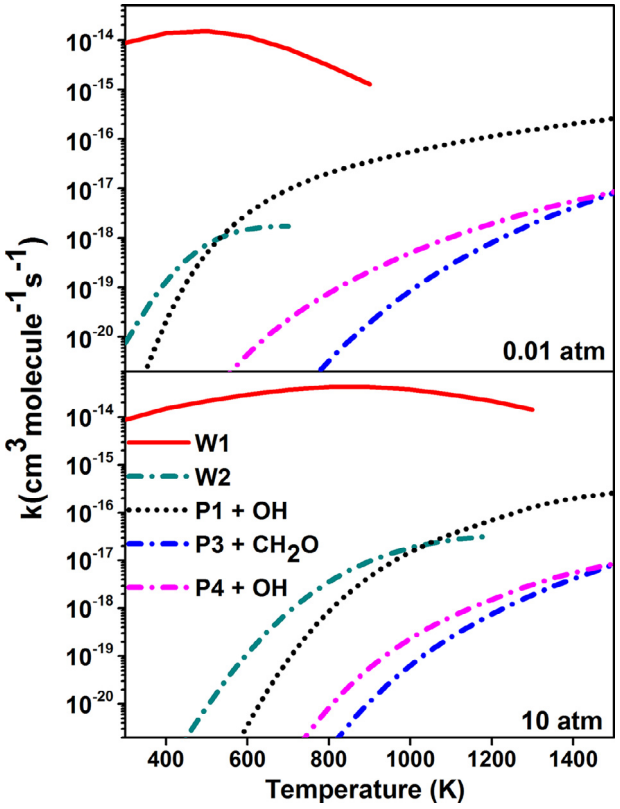


**Fig. 6.** Rate constants for MA2J + $O_2$ → products in the temperature range of 300–1500 K at 0.01 atm and 10 atm.

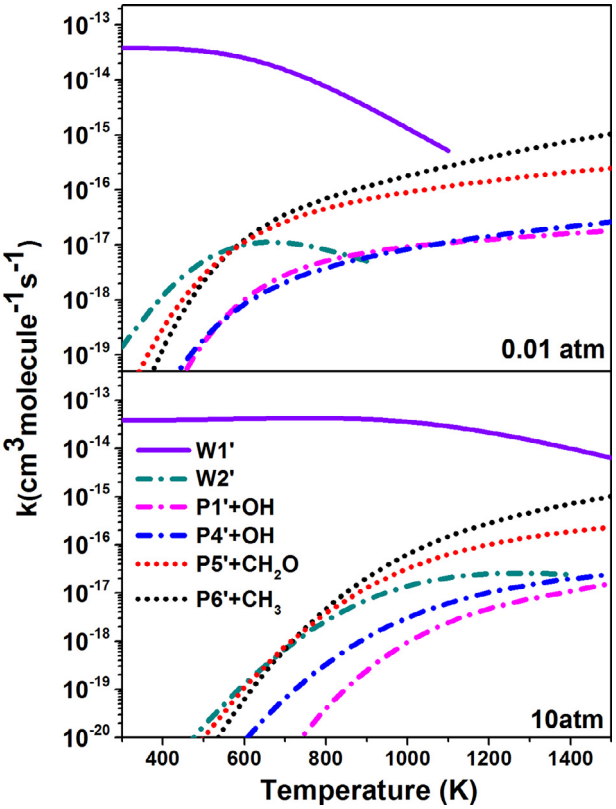


**Fig. 7.** Rate constants or MAMJ + $O_2$ → products in the temperature range 300–1500 K at 0.0 1atm and 10 atm.

To clearly clarify the relationship at various regimes (T/P), Figs. 6 and 7 display the temperature and pressure effect on the rate constants of main channels for two different systems. For simplicity, only rate constants at pressure of 0.01 atm and 10 atm were depicted in Figs. 6 and 7. The respective branching ratio of the production of MA2JOO and MAMJOO is sum up to 99% or more, indicating that the rate constants of stabilization reactions is 99% of the overall rate constant.

It is evident that the addition reaction MA2JOO formation is the most important channel and the OH elimination reaction is secondary, as shown in Fig. 6. Here the kinetic results confirm the observations made from the PES in Fig. 1. Our calculation also shows that the isomerization is not comparable with the re-dissociation reaction of MA2JOO radicals and the contribution of OH migration channel is negligible at low temperature. Both thermally and chemically activated formation of products become energetic and the formation of cyclic pathway is more competitive. The rate constant of stabilization reaction channel increases with pressure. Absence of rate constants at higher temperature is caused by multi-well reduction adopted in the MESS code. Furthermore, the rate constants of product channels decrease with increasing the pressure, and the similar trend for the $O_2$ addition to chain-like alkyl radical was observed. Comparing with other remaining channels, the rate constant of cyclization channel decreases faster. As shown in Fig. 7, the rate constant of the association reaction is the most favored reaction at the beginning stage and that of the isomerization reaction from MAMJOO to W2'is the secondary, which is consistent with the prediction based on PES in Fig. 1. With increasing pressure, the stabilization channel approaches the high-pressure limit at higher temperature. The rate constants of other channels generally decrease with increasing pressure. After $O_2$ addition reaction, these four channels competitive with each other subsequently. Our calculations show that the well depth of the initial adduct has great influence on the rate constants of consequent reactions. The dominant reaction channel is the formation of the initial adduct MAMJOO, as we anticipated. The reaction channel of aldehyde + OH formation is more competitive due to lower energy barrier. The rate constant of formaldehyde compounds channel is larger than that of isomerization, which can be attributed to the lower barrier heights of formaldehyde compounds channel. The isomerization and subsequent reaction channel play less important role in this system. The different temperature and pressure dependence observed in this system are consistent with the above discussion.

## 4. Conclusions

The chemistry of $O_2$ addition reactions in the low temperature oxidation of methyl acetate radicals has been theoretically investigated by using high-level ab initio method and transition state theory based on master equation analysis. The kinetic reaction network consisting of critical elementary reactions is constructed for the low temperature oxidation reactivity. The role of the $O_2$ addition reactions for both methyl acetate radicals has also been discussed. At temperature below 1000 K, the association reaction is most dominant of MA2J + $O_2$, and the cy[$OCH_2C(=O)OCH_2$] formation channel becomes more competitive with increasing temperature and pressure. As for reactions of MAMJ + $O_2$, a significant amount of $CH_3$ radicals are generated especially at higher temperatures. In addition, it should be noted that all the QOOH radicals are produced from methyl acetate peroxy radicals though isomerization reactions via 1, 6-H shift, which demonstrated that the H migration reactions have great influence on the low temperature oxidation reactivity of methyl acetate. Moreover, the predicted kinetic data for low-temperature oxidation of methyl acetate radicals

is believed to be helpful to improve the chemical kinetic modeling of methyl acetate oxidation.

## Acknowledgments

The work at University of Science and Technology of China was supported by, National Key Scientific Instruments and Equipment Development Program of China (2012YQ22011305), and National Natural Science Foundation of China (51676176, U1532137, 11575178 and 21373193). The work at the Hong Kong Polytechnic University was supported by RGC/ECS (PolyU 5380/13E), SRFDP and RGC ERG Joint Research Scheme (M-PolyU509/13), and NSFC (91641105). The authors thank the supercomputing service of the Supercomputing Center of University of Science and Technology of China.

## Supplementary materials

Supplementary material associated with this article can be found, in the online version, at doi:10.1016/j.combustflame.2018.05.023.

## References

[1] A.K. Agarwal, Biofuels (alcohols and biodiesel) applications as fuels for internal combustion engines, Prog. Energy Combust. Sci. 33 (2007) 233–271.
[2] J.Y.W. Lai, K.C. Lin, A. Violi, Biodiesel combustion: advances in chemical kinetic modeling, Prog. Energy Combust. Sci. 37 (2011) 1–14.
[3] K. Kohse-Höinghaus, P. Oßwald, T.A. Cool, T. Kasper, N. Hansen, F. Qi, C.K. Westbrook, P.R. Westmoreland, Biofuel combustion chemistry: from ethanol to biodiesel, Angew. Chem. Int. 49 (2010) 3572–3597.
[4] L.C. Meher, D. Vidya Sagar, S.N. Naik, Technical aspects of biodiesel production by transesterification—a review, Renew. Sustain. Energy Rev. 10 (2006) 248–268.
[5] Q. Feng, A. Jalali, A.M. Fincham, Y.L. Wang, T.T. Tsotsis, F.N. Egolfopoulos, Soot formation in flames of model biodiesel fuels, Combust. Flame 159 (2012) 1876–1893.
[6] Y. Zhai, B. Feng, W. Yuan, C. Ao, L. Zhang, Experimental and modeling studies of small typical methyl esters pyrolysis: methyl butanoate and methyl crotonate, Combust. Flame 191 (2018) 160–174.
[7] L. Yang, J.-y. Liu, Z.-s. Li, Theoretical studies of the reaction of hydroxyl radical with methyl acetate, J. Phys. Chem. A 112 (2008) 6364–6372.
[8] J.J. Orlando, G.S. Tyndall, The atmospheric oxidation of ethyl formate and ethyl acetate over a range of temperatures and oxygen partial pressures, Int. J. Chem. Kinet. 42 (2010) 397–413.
[9] X. Zhou, Y. Zhai, L. Ye, L. Zhang, Theoretical studies on the reaction kinetics of methyl crotonate with hydroxyl radical, Sustain. Energy Fuels (2018), doi:10.1039/C7SE00426E.
[10] S.M. Sarathy, S. Gaïl, S.A. Syed, M.J. Thomson, P. Dagaut, A comparison of saturated and unsaturated C4 fatty acid methyl esters in an opposed flow diffusion flame and a jet stirred reactor, Proc. Combust. Inst. 31 (2007) 1015–1022.
[11] S.L. Peukert, R. Sivaramakrishnan, M.C. Su, J.V. Michael, High temperature rate constants for H/D+methyl formate and methyl acetate, Proc. Combust. Inst. 34 (2013) 463–471.
[12] T. Tan, X. Yang, Y. Ju, E.A. Carter, Ab initio pressure-dependent reaction kinetics of methyl propanoate radicals, Phys. Chem. Chem. Phys. 17 (2015) 31061–31072.
[13] W. Ren, K.-Y. Lam, D.F. Davidson, R.K. Hanson, X. Yang, Pyrolysis and oxidation of methyl acetate in a shock tube: a multi-species time-history study, Proc. Combust. Inst. 36 (2017) 255–264.
[14] S. Dooley, H.J. Curran, J.M. Simmie, Autoignition measurements and a validated kinetic model for the biodiesel surrogate, methyl butanoate, Combust. Flame 153 (2008) 2–32.
[15] J. Zádor, C.A. Taatjes, R.X. Fernandes, Kinetics of elementary reactions in low-temperature autoignition chemistry, Prog. Energy Combust. Sci. 37 (2011) 371–421.
[16] P. Dagaut, N. Smoucovit, M. Cathonnet, Methyl acetate oxidation in a JSR: experimental and detailed kinetic modeling study, Combust. Sci. Technol. 127 (1997) 275–291.
[17] H. Tao, K.C. Lin, Pathways, kinetics and thermochemistry of methyl-ester peroxy radical decomposition in the low-temperature oxidation of methyl butanoate: a computational study of a biodiesel fuel surrogate, Combust. Flame 161 (2014) 2270–2287.
[18] Y. Jiao, F. Zhang, T.S. Dibble, Quantum chemical study of autoignition of methyl butanoate, J. Phys. Chem. A 119 (2015) 7282–7292.
[19] X. Yang, D. Felsmann, N. Kurimoto, J. Krüger, T. Wada, T. Tan, E.A. Carter, K. Kohse-Höinghaus, Y. Ju, Kinetic studies of methyl acetate pyrolysis and oxidation in a flow reactor and a low-pressure flat flame using molecular-beam mass spectrometry, Proc. Combust. Inst. 35 (2015) 491–498.
[20] R.C. Deka, B.K. Mishra, A theoretical investigation on the kinetics, mechanism and thermochemistry of gas-phase reactions of methyl acetate with chlorine atoms at 298 K, Chem. Phys. Lett. 595-596 (2014) 43–47.
[21] T. Tan, X. Yang, C.M. Krauter, Y. Ju, E.A. Carter, Ab initio kinetics of hydrogen abstraction from methyl acetate by hydrogen, methyl, oxygen, hydroxyl, and hydroperoxy radicals, J. Phys. Chem. A 119 (2015) 6377–6390.
[22] S. Jørgensen, V.F. Andersen, E.J.K. Nilsson, O.J. Nielsen, M.S. Johnson, Theoretical study of the gas phase reaction of methyl acetate with the hydroxyl radical: structures, mechanisms, rates and temperature dependencies, Chem. Phys. Lett. 490 (2010) 116–122.
[23] Y. Zhao, D.G. Truhlar, The M06 suite of density functionals for main group thermochemistry, thermochemical kinetics, noncovalent interactions, excited states, and transition elements: two new functionals and systematic testing of four M06-class functionals and 12 other functionals, Theor. Chem. Acc. 120 (2008) 215–241.
[24] I.M. Alecu, J. Zheng, Y. Zhao, D.G. Truhlar, Computational thermochemistry: scale factor databases and scale factors for vibrational frequencies obtained from electronic model chemistries, J. Chem. Theory Comput. 6 (2010) 2872–2887.
[25] H.-J. Werner, P.J. Knowles, G. Knizia, F.R. Manby, M. Schutz, and others, MOLPRO, version 2012.1 (2012). See http://www.molpro.net.
[26] D. Feller, D.A. Dixon, Extended benchmark studies of coupled cluster theory through triple excitations, J. Chem. Phys. 115 (2001) 3484–3496.
[27] J.G. Hill, K.A. Peterson, G. Knizia, H.J. Werner, Extrapolating MP2 and CCSD explicitly correlated correlation energies to the complete basis set limit with first and second row correlation consistent basis sets, J. Chem. Phys. 131 (2009) 194105.
[28] T. Shiozaki, G. Knizia, H.J. Werner, Explicitly correlated multireference configuration interaction: MRCI-F12, J, Chem. Phys. 134 (2011) 034113.
[29] K.A. Peterson, T.B. Adler, H.-J. Werner, Systematically convergent basis sets for explicitly correlated wavefunctions: the atoms H, He, B–Ne, and Al–Ar, J. Chem. Phys. 128 (2008) 084102.
[30] K.E. Yousaf, K.A. Peterson, Optimized complementary auxiliary basis sets for explicitly correlated methods: aug-cc-pVnZ orbital basis sets, Chem. Phys. Lett. 476 (2009) 303–307.
[31] L. Ye, L. Zhang, F. Qi, Ab initio kinetics on low temperature oxidation of iso-pentane: the first oxygen addition, Combust. Flame 190 (2018) 119–132.
[32] M.J. Frisch, G.W. Trucks, H.B. Schlegel, G.E. Scuseria, M.A. Robb, J.R. Cheeseman, G. Scalmani, V.Barone, B. Mennucci, G.A. Petersson, H. Nakatsuji, M. Caricato, Li X., H.P. Hratchian, A.F. Izmaylov, J.Bloino, Zheng G., J.L. Sonnenberg, M. Hada, M. Ehara, K. Toyota, R. Fukuda, J. Hasegawa, M. Ishida, T. Nakajima, Y. Honda, O. Kitao, H. Nakai, T. Vreven, J.J.A. Montgomery, J.E. Peralta, F. Ogliaro, M.Bearpark, J.J. Heyd, E. Brothers, K.N. Kudin, V.N. Staroverov, T. Keith, R. Kobayashi, J. Normand, K.Raghavachari, A. Rendell, J.C. Burant, S.S. Iyengar, J. Tomasi, M. Cossi, N. Rega, J.M. Millam, M. Klene, J.E. Knox, J.B. Cross, V. Bakken, C. Adamo, J. Jaramillo, R. Gomperts, R.E. Stratmann, O. Yazyev, A.J. Austin, R. Cammi, C. Pomelli, J.W. Ochterski, R.L. Martin, K. Morokuma, V.G.Zakrzewski, G.A. Voth, P. Salvador, J.J. Dannenberg, S. Dapprich, A.D. Daniels, O. Farkas, J.B.Foresman, J.V. Ortiz, J. Cioslowski, D.J. Fox Gaussian 09 Gaussian, Inc., Wallingford CT (2013).
[33] S.J. Klippenstein, J.A. Miller, From the time-dependent, multiple-well master equation to phenomenological rate coefficients, J. Phys. Chem. A 106 (2002) 9267–9277.
[34] Y. Georgievskii, J.A. Miller, M.P. Burke, S.J. Klippenstein, Reformulation and solution of the master equation for multiple-well chemical reactions, J. Phys. Chem. A 117 (2013) 12146–12154.
[35] L. Zhang, Q. Chen, P. Zhang, A theoretical kinetics study of the reactions of methylbutanoate with hydrogen and hydroxyl radicals, Proc. Combust. Inst. 35 (2015) 481–489.
[36] P. Zhang, S.J. Klippenstein, C.K. Law, Ab initio kinetics for the decomposition of hydroxybutyl and butoxy radicals of n-butanol, J. Phys. Chem. A 117 (2013) 1890–1906.
[37] H. Hippler, J. Troe, H. Wendelken, Collisional deactivation of vibrationally highly excited polyatomic molecules. II. Direct observations for excited toluene, J. Chem. Phys. 78 (1983) 6709–6717.
[38] T.H. Chung, M. Ajlan, L.L. Lee, K.E. Starling, Generalized multiparameter correlation for nonpolar and polar fluid transport properties, Ind. Eng. Chem. Res. 27 (1988) 671–679.
[39] T.H. Chung, L.L. Lee, K.E. Starling, Applications of kinetic gas theories and multiparameter correlation for prediction of dilute gas viscosity and thermal conductivity, Ind. Eng. Chem. Fundam. 23 (1984) 8–13.
[40] C. Eckart, The penetration of a potential barrier by electrons, Phys. Rev. 35 (1930) 1303–1309.
[41] J.A. Miller, S.J. Klippenstein, S.H. Robertson, A theoretical analysis of the reaction between ethyl and molecular oxygen, Proc. Combust. Inst. 28 (2000) 1479–1486.
[42] J.A. Miller, S.J. Klippenstein, The reaction between ethyl and molecular oxygen II: further analysis, Int. J. Chem. Kinet. 33 (2001) 654–668.
[43] S.J. Klippenstein, An efficient procedure for evaluating the number of available states within a variably defined reaction coordinate framework, J. Chem. Phys. 98 (1994) 11459–11464.
[44] J.A. Miller, Theory and modeling in combustion chemistry, Proc. Combust. Inst. 26 (1996) 461–480.
[45] G. da Silva, J.W. Bozzelli, Variational analysis of the phenyl + $O_2$ and phenoxy + O reactions, J. Phys. Chem. A 112 (2008) 3566–3575.

[46] O. Setokuchi, M. Sato, Direct dynamics of an alkoxy radical ($CH_3O$, $C_2H_5O$, and i-$C_3H_7O$) reaction with an oxygen molecule, J. Phys. Chem. A 106 (2002) 8124–8132.
[47] C. Fittschen, A. Frenzel, K. Imrik, P. Devolder, Rate constants for the reactions of $C_2H_5O$, i-$C_3H_7O$, and n-$C_3H_7O$ with NO and $O_2$ as a function of temperature, Int. J. Chem. Kinet. 31 (1999) 860–866.
[48] T. Yamada, J.W. Bozzelli, T. Lay, Thermodynamic and kinetic analysis using AB initio calculations on dimethyl-ether radical+$O_2$ reaction system, Proc. Combust. Inst. 27 (1998) 201–209.
[49] L.K. Rutz, G. da Silva, J.W. Bozzelli, H. Bockhorn, Reaction of the i-$C_4H_5$ ($CH_2CCHCH_2$) radical with $O_2$, J. Phys. Chem. A 115 (2011) 1018–1026.
[50] C.-J. Chen, J.W. Bozzelli, Thermochemical property, pathway and kinetic analysis on the reactions of allylic isobutenyl radical with $O_2$: an elementary reaction mechanism for isobutene oxidation, J. Phys. Chem. A 104 (2000) 9715–9732.
[51] H. Tao, K.C. Lin, Kinetic barriers, rate constants and branching ratios for unimolecular reactions of methyl octanoate peroxy radicals: a computational study of a mid-sized biodiesel fuel surrogate, Combust. Flame 180 (2017) 148–157.